Available online at http://scik.org
Commun. Math. Biol. Neurosci. 2025, 2025:116
https://doi.org/10.28919/cmbn/9505
ISSN: 2052-2541

APPROXIMATE BAYESIAN COMPUTATION FOR THE ROSS-MACDONALD MODEL OF MALARIA TRANSMISSION

A. OKWOMI SHARON[1,*], SAMUEL CHEGE MAINA[1,2], COLLINS OJWANG' ODHIAMBO[1,3], SAMUEL MWALILI[1]

[1]Strathmore Institute for Mathematical Sciences, Strathmore University, Nairobi, Kenya

[2]Microsoft Research Lab – Africa, Nairobi, Kenya

[3]Department of Paediatrics, College of Medicine, University of Illinois, Peoria, IL, United States

Abstract. The Ross-Macdonald model remains a key component in understanding the dynamics of malaria transmission, representing the complex interactions between mosquito and human populations through a coupled system of ordinary differential equations (ODEs). Parameter estimation for this model presents significant challenges due to the intractable likelihood function and multiple uncertain parameters that govern transmission dynamics in epidemiology. This study implements Approximate Bayesian Computation with Sequential Monte Carlo (ABC-SMC) methods to perform parameter inference on the Ross-Macdonald model. We demonstrate that ABC-SMC provides a robust framework for parameter estimation while accounting for model uncertainty and parameter correlations. Our analysis reveals critical information on the sensitivity of the basic reproduction number R_0 to various epidemiological parameters. The methodology presented offers a practical approach to the development of evidence-based policies and provides uncertainty quantification essential for robust decision making.

Keywords: Markov chains; sequential Monte Carlo; Bayesian inference; Bayes rule.

2020 AMS Subject Classification: 34C60.

*Corresponding author

E-mail address: sharonokwomi@gmail.com

Received July 23, 2025

1. INTRODUCTION

Malaria remains a significant public health challenge worldwide, with an estimated 263 million cases and 597,000 deaths worldwide in the year 2023 [1]. The disease disproportionately affects sub-Saharan Africa, which accounts for approximately 94% of global cases and 95% of malaria-related deaths [2]. Kenya represents a particularly compelling case study, with 75% of its population at risk and an estimated 3.3 million malaria cases in 2023 [3, 4]. Despite significant investments in malaria control measures including insecticide-treated bed nets (ITNs), indoor residual spraying, and antimalarial treatments, transmission persists in endemic regions, highlighting the need for sophisticated mathematical models to guide intervention strategies.

The Ross-Macdonald model, originally developed by Ronald Ross in the early twentieth century and subsequently refined by George Macdonald in the 1950s, serves as a fundamental framework for understanding malaria transmission dynamics [5, 6]. This model captures the essential features of malaria transmission through a system of coupled ODEs that describe the proportions of infected individuals in both human and mosquito populations. The model's enduring relevance stems from its ability to incorporate key biological and epidemiological processes while maintaining mathematical tractability. The standard Ross-Macdonald model is formulated as [7], [8]:

$$\begin{aligned} \dot{I_h} &= abmI_m(1-I_h) - rI_h \\ \dot{I_m} &= acI_h(1-I_m) - \mu_m I_m \end{aligned} \tag{1}$$

TABLE 1. Table showing typical parameter ranges of $\mathscr{M}_0$ model, [7].

Parameter	Description	Typical Range
a	Man biting rate/day	$[0.01, 0.5]$
b	Proportion of bites that produces an infection in humans	$[0.2, 0.5]$
c	Proportion of bites by which one susceptible mosquito becomes infected	$[0.5]$
m	Female mosquito-human ratio	$[0.5, 40]$
r	Average recovery rate/day of humans	$[0.005, 0.05day]$
μ	Per capita rate/day of mosquito mortality	$[0.05, 0.5]$

where $I_h$and I_m represent the proportions of infected humans and mosquitoes, respectively, and the parameters a, b, c, m, r, and μ_m capture various aspects of the transmission process as shown in Table 1. The basic reproduction number, $R_0 = ma^2bc/r\mu$. R_0, serves as a critical threshold parameter that determines whether malaria will persist $(R_0 > 1)$ or fade out $(R_0 < 1)$ in a population.

Despite its conceptual elegance, parameter estimation for the Ross-Macdonald model presents substantial challenges. Traditional likelihood-based methods are often impractical due to the complex nature of epidemiological data, measurement errors, and the intractable likelihood function arising from stochastic observation processes. Furthermore, many model parameters are difficult to measure directly in field settings, leading to significant uncertainty in parameter values. Approximate Bayesian Computation (ABC) has emerged as a powerful alternative to traditional likelihood-based inference methods, particularly suited for complex models where the likelihood function is computationally intractable or unavailable [9, 10]. ABC methods bypass the need for explicit likelihood evaluation by comparing simulated data from the model with observed data using summary statistics and distance metrics. When combined with Sequential Monte Carlo (SMC) algorithms, ABC provides an efficient framework to explore high-dimensional parameter spaces while maintaining computational feasibility [11, 12].

The ABC approach has gained considerable traction in infectious disease modeling, offering a suite of model fitting methods that circumvent the need for explicit likelihood functions. ABC methods have proven especially valuable for ODE models in epidemiology, where traditional Bayesian approaches may become computationally intractable. Among ABC implementations, Sequential Monte Carlo approaches ABC-SMC have demonstrated superior performance compared to rejection-based and Markov Chain Monte Carlo variants. ABC-SMC algorithms achieve computational efficiency improvements through adaptive tolerance schedules and importance sampling, while maintaining the ability to explore complex posterior surfaces. The sequential nature of SMC allows for progressive approximation of the posterior distribution through a series of intermediate target distributions, starting from the prior and converging toward the true posterior. Furthermore, perturbation kernel optimization in ABC-SMC can yield

substantial computational efficiency gains, with locally adapted kernels often showing superior performance for complex posterior distributions [13].

The application of ABC methods to malaria modeling has shown considerable promise, though systematic applications to the Ross-Macdonald framework remain limited. Recent comparative studies of approximate versus exact Bayesian techniques in epidemiological ODE models, including applications to malaria transmission data from Afghanistan, have highlighted both the potential and limitations of ABC approaches [14]. Key considerations for effective ABC implementation in infectious disease contexts include algorithm choice, perturbation variance optimization, and summary statistic selection.

Contemporary developments in ABC methodology continue to enhance its applicability to complex epidemiological systems. Recent advances in Sequential Monte Carlo methods, including online variants that process data sequentially with fixed observation windows, offer potential for real-time epidemic monitoring and parameter updating. Applications to COVID-19 modelling have demonstrated the feasibility of ABC-SMC approaches for estimating time-varying reproduction numbers in realistic epidemiological settings [15], suggesting broader applicability to malaria transmission modelling with temporal parameter variation.

This study contributes to the growing literature on ABC methods in epidemiological modelling by presenting a comprehensive application to the Ross-Macdonald model. Our objectives are threefold: (1) to demonstrate the practical implementation of ABC-SMC for parameter estimation in the Ross-Macdonald model, (2) to quantify parameter uncertainty and investigate parameter correlations that influence malaria transmission dynamics, and (3) to assess the sensitivity of key epidemiological indicators to model parameters.

1.1. Introduction. We consider the Ross-Macdonald model, which describes malaria transmission through a system of two coupled ODEs that represent the dynamics of proportions infected in human and mosquito populations. The model assumes homogeneous mixing between populations and incorporates key biological parameters that govern transmission rates and recovery processes. Equation (1) captures the rate of change in the proportion of infected humans I_h, where new infections occur through contact with infected mosquitoes at a rate $abmI_m(1-I_h)$, and recovery occurs at a rate rI_h. The mosquito equation (2) describes the dynamics of infected

mosquitoes (I_m), with new infections occurring through blood meals of infected humans at a rate $acI_h(1-I_m)$, and mosquito mortality removing infected individuals at a rate $\mu_m I_m$.

1.2. Bayesian Inference. The Bayesian approach frames the unknown model parameters as random variables with associated probability distributions representing uncertainty. Using Bayes' theorem,these prior distributions are updated based on the likelihood of observed data with different parameter values, resulting in posterior distributions [16]. Computationally intensive methods such as MCMC are often required to generate samples from the posterior to approximate it [17]. The posterior encapsulates the updated belief in the parameters after conditioning on the data, providing a basis for estimation and prediction [18].

Let $\mathbf{X}(t) = (S_h(t), I_h(t), R_h(t), S_m(t), I_m(t))$ denote the state variables, and let $\theta = (\alpha_h, \alpha_m, \beta_h, \beta_m, \gamma_h, \rho_h, \delta_h, \pi_h, \pi_m)$ denote the parameter vector. Given observations $\mathbf{D}$ (e.g., time-series data of $I_h(t)$), our goal is to estimate the posterior distribution:

$$P(\theta \mid \mathbf{D}) \propto P(\mathbf{D} \mid \theta) \cdot P(\theta).$$

Due to the intractability of the likelihood function $P(\mathbf{D} \mid \theta)$, we apply Approximate Bayesian Computation (ABC).

1.3. Approximate Bayesian Computation Algorithms. Approximate Bayesian Computation (ABC) approximates the posterior distribution using simulation and rejection based on distance from the observed data.

i. Sample $\theta^{(i)} \sim P(\theta)$ from the prior.

ii. Simulate the system Eq (1) using numerical integration (e.g., Runge-Kutta) to obtain simulated data $\mathbf{D}^{(i)}$.

iii. Compute a distance between simulated and observed data:

$$\rho(\mathbf{D}^{(i)}, \mathbf{D}) = \sqrt{\sum_t \left(I_h^{(i)}(t) - I_h^{\text{obs}}(t) \right)^2}.$$

iv. Accept $\theta^{(i)}$ if $\rho(\mathbf{D}^{(i)}, \mathbf{D}) < \varepsilon$.

The set of accepted parameters approximates the posterior distribution:

$$P(\theta \mid \rho < \varepsilon).$$

More efficient algorithms include:

a. **ABC-MCMC:** Combines ABC with Metropolis-Hastings sampling.
b. **ABC-SMC:** Uses sequential Monte Carlo sampling to iteratively refine samples using decreasing tolerances ε_t.

1.3.1. *ABC-MCMC: Approximate Bayesian Computation with Metropolis-Hastings.* Approximate Bayesian Computation with Metropolis-Hastings (ABC-MCMC) is an algorithm that combines ABC rejection with the Markov Chain Monte Carlo (MCMC) framework to improve sampling efficiency from the approximate posterior distribution, especially in high-dimensional settings.

In standard ABC rejection, parameter values are independently drawn from the prior, which becomes highly inefficient as the parameter dimension increases or when the acceptance threshold ε is small. ABC-MCMC addresses this limitation by exploring the parameter space using MCMC and accepting proposed parameters based on how well they reproduce the observed data.

Let $\theta \in \Theta$ be the parameter vector of interest,$\pi(\theta)$ be the prior distribution over Θ, $\mathbf{D}^{\text{obs}}$ be the observed data, $\mathbf{D}' \sim \mathscr{M}(\theta)$ be data simulated from the model given θ, $\rho(\mathbf{D}', \mathbf{D}^{\text{obs}})$ be a distance metric between simulated and observed data,$q(\theta' \mid \theta)$ be a proposal distribution for the MCMC algorithm and $\varepsilon > 0$ be the tolerance threshold.

Given an initial value $\theta^{(0)}$, a general ABC-MCMC algorithm proceeds as follows:

Algorithm 1 General ABC-MCMC Algorithm

for $i = 0, 1, \ldots, N-1$ **do**

  Propose a new parameter vector:

$$\theta' \sim q(\cdot \mid \theta^{(i)}).$$

  Simulate data $\mathbf{D}'$ from the model using θ'.

  Compute the distance:

$$\rho = \rho(\mathbf{D}', \mathbf{D}^{\text{obs}}).$$

  if $\rho < \varepsilon$ **then**

    Compute the Metropolis-Hastings acceptance probability:

$$\alpha = \min\left(1, \frac{\pi(\theta')\, q(\theta^{(i)} \mid \theta')}{\pi(\theta^{(i)})\, q(\theta' \mid \theta^{(i)})}\right).$$

    With probability α, accept the proposal:

$$\theta^{(i+1)} = \theta', \quad \text{else } \theta^{(i+1)} = \theta^{(i)}.$$

  else

    Reject and set:

$$\theta^{(i+1)} = \theta^{(i)}.$$

  end if

end for

In ABC-MCMC, the proposal distribution $q(\theta' \mid \theta)$ is often chosen to be symmetric, such as a Gaussian random walk, to simplify the acceptance probability calculation. The choice of the tolerance level ε plays a crucial role: smaller values yield more accurate approximations to the true posterior but at the cost of lower acceptance rates and increased computational effort, whereas larger values lead to faster sampling but poorer approximation. The resulting posterior distribution that is sampled via ABC-MCMC is an approximation of the true posterior, conditioned on the simulated data being sufficiently close to the observed data, specifically within the threshold *varepsilon*, that is,

$$P(\theta \mid \rho(\mathbf{D}', \mathbf{D}^{\text{obs}}) < \varepsilon).$$

ABC-MCMC offers several advantages over basic ABC rejection, particularly in high-dimensional parameter spaces. It is more efficient and allows the use of MCMC diagnostics

such as trace plots and autocorrelation functions to assess convergence. Moreover, the MCMC framework enables exploration of complex posterior surfaces. However, the method also has limitations: it can be computationally intensive due to the need for repeated forward simulations of the model. The algorithm requires careful tuning of both the proposal distribution and the tolerance threshold *varepsilon*. If *varepsilon* is too small, the acceptance rate may be prohibitively low, while a large *varepsilon* undermines the quality of the posterior approximation.

We aim to estimate the posterior distribution of parameters $\theta = (a, b, c, m, r, \mu_m)$ given observed data D_{obs}, using ABC-MCMC for the Ross-Macdonald Model.

Algorithm 2 ABC-MCMC for Ross-Macdonald Model

Input: Prior distribution $\pi(\theta)$, tolerance ε, observed data D_{obs}, proposal distribution $q(\theta'|\theta)$, total iterations N.

Initialize: Draw initial $\theta^{(0)}$ from $\pi(\theta)$, simulate $D^{(0)} \sim M(\theta^{(0)})$, set $i = 0$.

for $i = 0$ to $N-1$ **do**

Propose a new parameter vector $\theta' \sim q(\cdot \mid \theta^{(i)})$.

Simulate the Ross-Macdonald model using θ' to obtain simulated data D':

$$\frac{dI_h}{dt} = abmI_m(1-I_h) - rI_h,$$
$$\frac{dI_m}{dt} = acI_h(1-I_m) - \mu_m I_m.$$

Compute the distance between simulated and observed data:

$$\rho = \sqrt{\sum_t \left(I_h'(t) - I_h^{\text{obs}}(t)\right)^2}.$$

if $\rho < \varepsilon$ **then**

Compute the Metropolis-Hastings acceptance probability:

$$\alpha = \min\left(1, \frac{\pi(\theta')\, q(\theta^{(i)}|\theta')}{\pi(\theta^{(i)})\, q(\theta'|\theta^{(i)})}\right).$$

With probability α, accept θ' and set $\theta^{(i+1)} = \theta'$, otherwise $\theta^{(i+1)} = \theta^{(i)}$.

else

Reject θ' and set $\theta^{(i+1)} = \theta^{(i)}$.

end if

end for

Output: Posterior sample $\{\theta^{(i)}\}_{i=1}^{N}$ approximating $P(\theta \mid \rho(D', D_{\text{obs}}) < \varepsilon)$.

1.3.2. *ABC-SMC: Approximate Bayesian Computation with Sequential Monte Carlo.* Approximate Bayesian Computation via Sequential Monte Carlo (ABC-SMC) is a likelihood-free inference method that refines posterior estimates by progressing through a sequence of intermediate distributions with decreasing tolerance levels. It is especially suitable for high-dimensional models or those with intractable likelihoods but feasible forward simulation.

Let $\theta \in \Theta$ denote the vector of model parameters, $\pi(\theta)$ denote the prior distribution, $\mathbf{D}^{\text{obs}}$ be the observed data, $\mathscr{M}(\theta)$ be the stochastic/deterministic model from which data $\mathbf{D}$ can be simulated, $\rho(\mathbf{D}, \mathbf{D}^{\text{obs}})$ be a distance function between simulated and observed data, ε_t be the tolerance at generation t and $K_t(\cdot \mid \cdot)$ be the perturbation kernel at generation t.

Algorithm 3 General ABC-SMC Algorithm: Iterations for Generation $t \geq 2$

1: **for** $i = 1$ to N **do**

2: Resample $\theta_{t-1}^{(j)}$ with probability $\tilde{w}_{t-1}^{(j)}$.

3: Perturb the resampled parameter:

$$\theta_t^{(i)} \sim K_t(\cdot \mid \theta_{t-1}^{(j)}).$$

4: Simulate data from the model:

$$\mathbf{D}^{(i)} \sim \mathscr{M}(\theta_t^{(i)}).$$

5: Accept $\theta_t^{(i)}$ if:

$$\rho(\mathbf{D}^{(i)}, \mathbf{D}^{\text{obs}}) < \varepsilon_t.$$

6: Compute the importance weight:

$$w_t^{(i)} = \frac{\pi(\theta_t^{(i)})}{\sum_{j=1}^{N} \tilde{w}_{t-1}^{(j)} K_t(\theta_t^{(i)} \mid \theta_{t-1}^{(j)})}.$$

7: **end for**

8: Normalize the weights:

$$\tilde{w}_t^{(i)} = \frac{w_t^{(i)}}{\sum_{j=1}^{N} w_t^{(j)}}.$$

The distribution at generation t approximates:

$$P_t(\theta) \approx P(\theta \mid \rho(\mathbf{D}, \mathbf{D}^{\text{obs}}) < \varepsilon_t),$$

with convergence to the true posterior as $\varepsilon_t \to 0$.

ABC-SMC offers several advantages, including the efficient reuse of previously accepted particles through resampling and importance weighting, which improves computational efficiency. It provides a better approximation to the posterior distribution compared to basic ABC rejection by progressively refining the particle population over generations. Its adaptive nature—enabled by decreasing tolerance thresholds and appropriately chosen kernel bandwidths—allows the algorithm to gradually concentrate on regions of high posterior density. However, ABC-SMC also presents challenges: it requires careful tuning of both the tolerance schedule ε_t and the perturbation kernel K_t, is computationally demanding due to repeated simulations and weight calculations, and its performance is sensitive to the choice of distance function ρ, which must appropriately capture similarity between simulated and observed data.

We aim to estimate the posterior distribution of the Ross-Macdonald model parameters $\theta = (a, b, c, m, r, \mu_m)$ using ABC-SMC as described in [7]. Let ε_t be the tolerance at generation t, $q_t(\cdot|\cdot)$ the perturbation kernel, and $\rho(D, D_{\text{obs}})$ the distance between simulated and observed data.

Algorithm 4 ABC-SMC for Ross-Macdonald Model

Input: Prior $\pi(\theta)$, tolerances $\{\varepsilon_t\}_{t=1}^{T}$, observed data D_{obs}, number of particles N, perturbation kernels $K_t(\cdot|\cdot)$.

Output: Weighted particles $\{\theta_t^{(i)}, w_t^{(i)}\}_{i=1}^{N}$ approximating $P(\theta|\rho(D, D_{\text{obs}}) < \varepsilon_t)$.

Initialization: $t = 1$

for $i = 1$ to N **do**

  repeat

    Sample $\theta_1^{(i)} \sim \pi(\theta)$.

    Simulate $D^{(i)} \sim M(\theta_1^{(i)})$ using the Ross-Macdonald system:

$$\frac{dI_h}{dt} = abmI_m(1 - I_h) - rI_h,$$
$$\frac{dI_m}{dt} = acI_h(1 - I_m) - \mu_m I_m.$$

    Compute distance:

$$\rho(D^{(i)}, D_{\text{obs}}) = \sqrt{\sum_t (I_h^{(i)}(t) - I_h^{\text{obs}}(t))^2}$$

  until $\rho(D^{(i)}, D_{\text{obs}}) < \varepsilon_1$

  Set weight $w_1^{(i)} = 1$.

end for

Normalize weights:

$$\tilde{w}_1^{(i)} = \frac{w_1^{(i)}}{\sum_{j=1}^{N} w_1^{(j)}}$$

Sequential Iterations: For $t = 2, \ldots, T$

for $i = 1$ to N **do**

  repeat

    Resample $\theta_{t-1}^{(j)}$ with probability $\tilde{w}_{t-1}^{(j)}$.

    Perturb: $\theta_t^{(i)} \sim K_t(\cdot|\theta_{t-1}^{(j)})$.

    Simulate $D^{(i)} \sim M(\theta_t^{(i)})$ via Ross-Macdonald dynamics.

    Compute distance $\rho(D^{(i)}, D_{\text{obs}})$.

  until $\rho(D^{(i)}, D_{\text{obs}}) < \varepsilon_t$

  Compute importance weight:

$$w_t^{(i)} = \frac{\pi(\theta_t^{(i)})}{\sum_{j=1}^{N} \tilde{w}_{t-1}^{(j)} K_t(\theta_t^{(i)}|\theta_{t-1}^{(j)})}$$

end for

Normalize weights:

$$\tilde{w}_t^{(i)} = \frac{w_t^{(i)}}{\sum_{j=1}^{N} w_t^{(j)}}$$

The ABC-SMC algorithm progressively refines posterior estimates by decreasing the tolerance levels ε_t over iterations. As $t \to T$ and $\varepsilon_T \to 0$, the distribution of particles converges to the true posterior:

$$P(\theta|\rho(D, D_{\text{obs}}) < \varepsilon_T).$$

1.4. Diagnostic Measures.

1.4.1. *Effective Sample Size (ESS).* The **Effective Sample Size (ESS)** measures how many *independent* samples a posterior sample is approximately equivalent to. Although a Markov chain or Sequential Monte Carlo (SMC) procedure may generate N samples or particles, correlations between samples (MCMC) or unequal particle weights (SMC) reduce the effective information content.

ESS in ABC-MCMC. In Markov Chain Monte Carlo (MCMC), samples are autocorrelated, which reduces the efficiency of posterior exploration. The ESS is estimated as:

$$ESS_{\text{MCMC}} \approx \frac{N}{1 + 2\sum_{k=1}^{\infty} \rho_k},$$

where N is the number of posterior samples after burn-in and ρ_k is the lag-k autocorrelation of the Markov chain. A well-mixed chain has low autocorrelation ($\rho_k \to 0$), giving $ESS \approx N$, while high autocorrelation drastically lowers the ESS.

ESS in ABC-SMC. In Sequential Monte Carlo (SMC), samples are independent but have associated importance weights. The ESS is computed from the normalized weights (w_i) as:

$$ESS_{\text{SMC}} = \frac{1}{\sum_{i=1}^{N} w_i^2}.$$

When weights are nearly uniform ($w_i \approx 1/N$), $ESS \approx N$, indicating that most particles contribute effectively. If weights are highly concentrated (a few particles dominate),$ESS \ll N$.

1.4.2. *Acceptance Rate and Mean Posterior Variance.*

Acceptance Rate. The **Acceptance Rate** quantifies the proportion of proposals (MCMC) or particles (SMC) that are accepted during posterior approximation.

In ABC-MCMC. The acceptance rate is computed as:

$$\text{Acceptance Rate} = \frac{\text{Number of Accepted Proposals}}{\text{Total Number of Proposals}}.$$

A very low acceptance rate (e.g., < 0.1) indicates poor mixing due to a strict tolerance ε or poorly tuned proposal distribution, while a very high rate (e.g., > 0.6) may imply that ε is too loose, leading to biased posterior approximations. A desirable range is typically 0.2–0.4, balancing posterior accuracy and efficient exploration.

In ABC-SMC. The acceptance rate is reported per generation:

$$\text{Acceptance Rate}_t = \frac{\text{Particles Accepted at Generation } t}{\text{Total Proposals at Generation } t}.$$

As the tolerance ε_t decreases across generations, the acceptance rate usually declines. A non-negligible acceptance rate in the final generation suggests a reasonable trade-off between efficiency and posterior accuracy.

Mean Posterior Variance. The **Mean Posterior Variance** summarizes posterior uncertainty across all parameters. For parameters $\theta = (\theta_1, \ldots, \theta_p)$:

$$\text{Mean Posterior Variance} = \frac{1}{p}\sum_{k=1}^{p} \text{Var}(\theta_k \mid \text{data}).$$

A smaller posterior variance indicates increased concentration of the posterior mass around plausible parameter values, reflecting more precise estimates. However, overly small variance may indicate underestimation of uncertainty if ε is too strict.

2. Simulation Study

To perform an ABC analysis, we define a prior distribution for each of the parameters and the initial state, and generate a set of parameter values and initial conditions from these prior distributions. We then simulate the Ross model using these parameter values and initial conditions, and compare the synthetic data to the observed data to calculate a summary statistic. We repeat this process many times to generate a set of summary statistics, and accept the parameter values and initial conditions that result in summary statistics that are close enough to the observed data.

TABLE 2. Comparison of ABC-MCMC and ABC-SMC Estimates

Parameter	True Value	ABC-MCMC Mean ± SD	ABC-SMC Mean ± SD
a	0.5	0.4278 ± 0.1599	0.5091 ± 0.0938
b	0.3	0.4989 ± 0.2343	0.5135 ± 0.1490
c	0.2	0.4827 ± 0.2377	0.4105 ± 0.1083
m	5.0	6.4368 ± 1.7042	2.4091 ± 1.0036
r	0.1	0.2687 ± 0.1243	0.1321 ± 0.0773
μ_m	0.2	0.2840 ± 0.1236	0.3000 ± 0.0894

Figure 1 compares posterior densities obtained using Approximate Bayesian Computation with Markov Chain Monte Carlo (ABC-MCMC) and Approximate Bayesian Computation with Sequential Monte Carlo (ABC-SMC) for six parameters: a, b, c, m, r, and μ_m. The blue curves represent ABC-MCMC while the green curves represent ABC-SMC, with dashed vertical lines indicating posterior means.

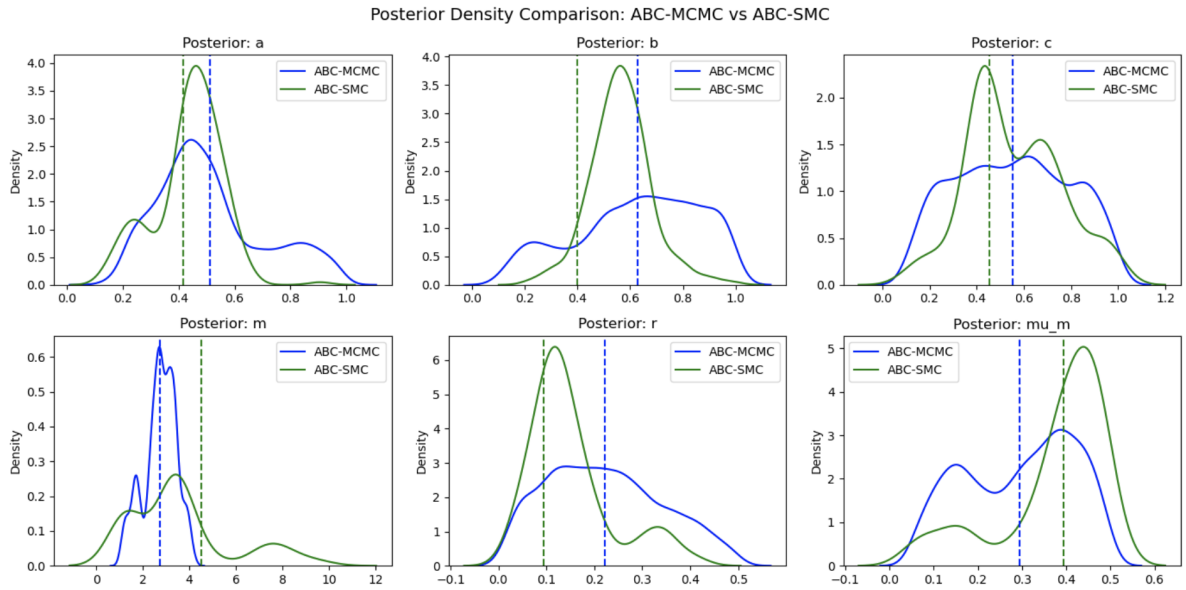

FIGURE 1. Posterior Density Comparing ABC-MCMC vs ABC-SMC

For parameter a, both methods yield unimodal posterior distributions with similar central tendencies, although ABC-SMC produces a slightly narrower distribution, indicating higher precision and better concentration around the mean. Parameter b shows a similar trend, where

ABC-SMC exhibits a sharper peak and reduced posterior uncertainty, whereas ABC-MCMC produces a flatter distribution. For parameter c, both methods agree closely on the posterior mean, though ABC-SMC again demonstrates slightly greater precision.

More pronounced differences are observed for parameter m. ABC-MCMC presents a sharp unimodal posterior centered around $m \approx 4$, while ABC-SMC reveals a broader, slightly bimodal distribution, suggesting exploration of multiple plausible parameter regions. Parameter r also shows clear differences: ABC-SMC provides a sharply peaked posterior around $r \approx 0.1$, indicating better identifiability, whereas ABC-MCMC produces a wider distribution, reflecting higher uncertainty. For μ_m, ABC-SMC yields a bimodal posterior, suggesting possible parameter identifiability challenges or underlying model complexity, whereas ABC-MCMC smooths over this multimodality, resulting in a unimodal posterior.

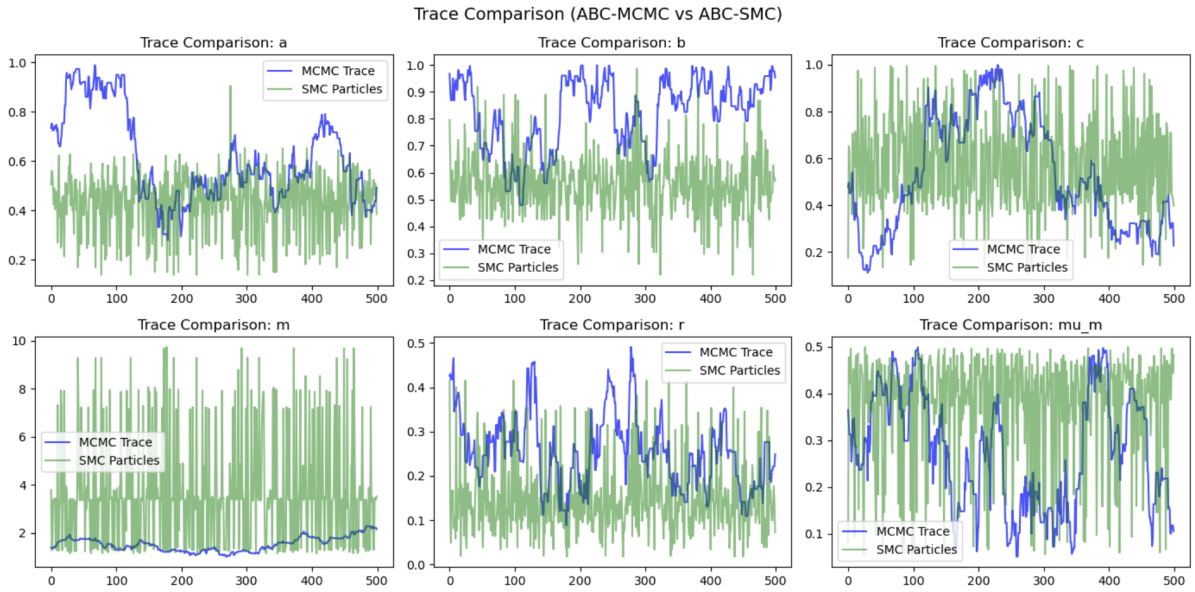

FIGURE 2. Trace plot Comparing ABC-MCMC vs ABC-SMC

Figure 2 presents trace plots comparing parameter sampling using Approximate Bayesian Computation with Markov Chain Monte Carlo (ABC-MCMC) and Approximate Bayesian Computation with Sequential Monte Carlo (ABC-SMC) for six parameters: a, b, c, m, r, and μ_m. The blue lines represent MCMC traces, while the green lines denote SMC particles. Trace plots provide insight into mixing efficiency, convergence, and posterior space exploration.

For parameter a, ABC-MCMC exhibits slow movement with strong autocorrelation and delayed exploration of the posterior space, indicating poor mixing. In contrast, ABC-SMC particles fluctuate broadly across iterations, demonstrating more efficient exploration. A similar pattern is observed for parameter b, where the MCMC trace remains stationary for long periods, suggesting limited exploration, while ABC-SMC shows greater variability and improved posterior sampling. For parameter c, both methods explore the posterior, but ABC-MCMC transitions more slowly between regions, whereas ABC-SMC displays rapid fluctuations and better coverage.

Notable differences appear for parameter m, where the MCMC trace is nearly flat, indicating possible convergence to a local mode and limited exploration. ABC-SMC particles vary widely, consistent with the bimodal posterior observed earlier, suggesting effective sampling of multiple high-probability regions. For parameter r, ABC-MCMC again shows high autocorrelation, while ABC-SMC transitions rapidly, indicating more efficient mixing. The same trend is evident for μ_m, where ABC-SMC explores the parameter space dynamically, in contrast to ABC-MCMC's slower convergence.

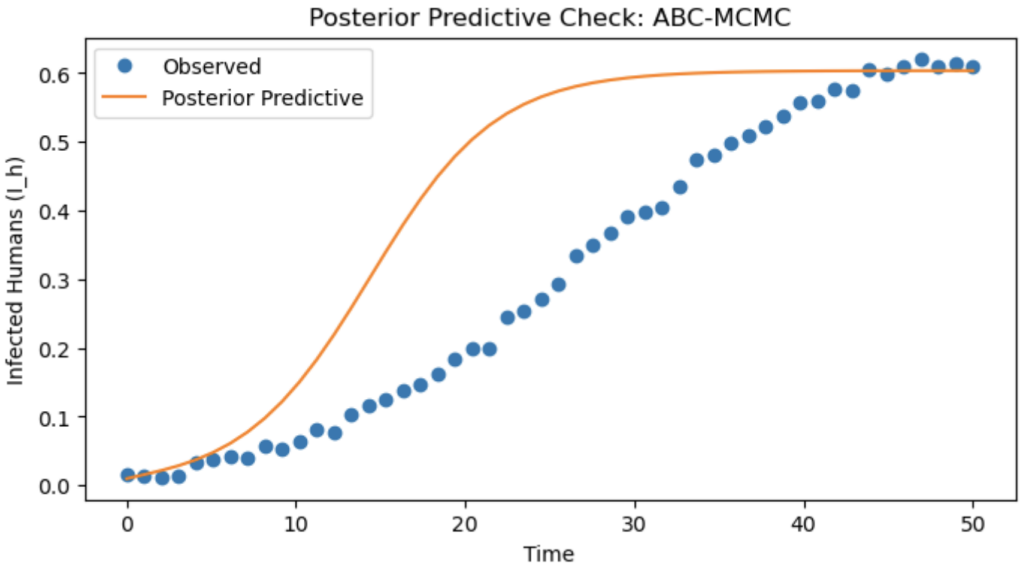

FIGURE 3. Posterior Predictive Check of ABC-MCMC

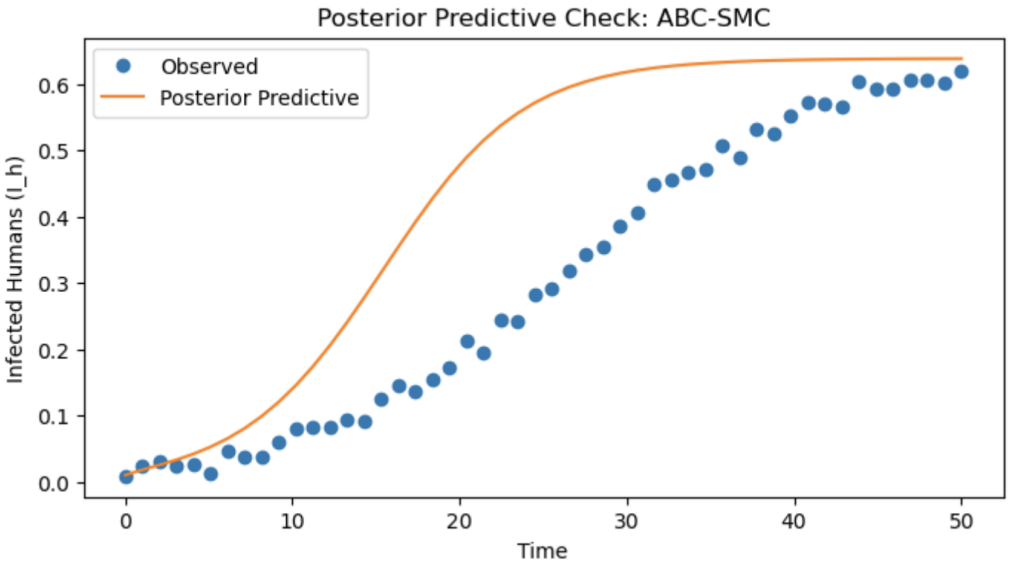

FIGURE 4. Posterior Predictive Check of ABC-SMC

Figures 3 and 4 present posterior predictive checks for the ABC-MCMC and ABC-SMC methods, respectively. The blue dots represent observed data for the proportion of infected humans (I_h) over time, while the orange lines indicate the posterior predictive means. Posterior predictive checks are used to assess model adequacy by evaluating how well the inferred posterior reproduces the observed epidemic trajectory.

For ABC-MCMC (Figure 3), the posterior predictive curve captures the general epidemic trend, correctly reflecting the initial exponential growth and the eventual plateau phase. However, it slightly underestimates infection levels during the mid-epidemic period (approximately time 15–30) and reaches the plateau earlier than observed. This discrepancy suggests that the posterior obtained via ABC-MCMC may be biased toward faster epidemic dynamics, which is consistent with its poorer posterior exploration and higher autocorrelation identified in the trace plots.

The ABC-SMC posterior predictive (Figure 4) similarly replicates the overall epidemic pattern but shows improved agreement during the mid-epidemic phase. The infections are more accurately reproduced in the growth phase, indicating that ABC-SMC better captures the underlying transmission dynamics. Nonetheless, the ABC-SMC predictions slightly underestimate

infections in the late epidemic phase (time 40–50), where observed infection levels remain marginally higher than the predictive mean.

As shown in Table 3, ABC-SMC often yields lower posterior variance due to adaptive tolerance reduction and weighted particle resampling, whereas ABC-MCMC may retain higher variance when mixing is poor or acceptance rates are very low. A high ESS (close to N) indicates good posterior exploration and minimal degeneracy. Thus, ABC-SMC typically achieves higher ESS per particle, while ABC-MCMC may require longer runs or thinning to achieve similar efficiency.

TABLE 3. Comparison of ABC-MCMC and ABC-SMC Diagnostics

Diagnostic	ABC-MCMC	ABC-SMC
Acceptance Rate	0.250	0.310
Mean Posterior Variance	0.5120	0.1457
ESS (Final)	312.0	2.4

3. CONCLUSION

The comparative evaluation of ABC-MCMC and ABC-SMC methods highlights distinct differences in posterior inference, mixing efficiency, and predictive performance. The posterior density plots indicate that ABC-SMC generally produces sharper and more concentrated posterior distributions, reflecting improved parameter identifiability and reduced uncertainty. In contrast, ABC-MCMC yields wider and smoother distributions, suggesting higher uncertainty and possible convergence to local modes. The bimodal posteriors observed for some parameters under ABC-SMC, such as m and μ_m, demonstrate its ability to explore multiple high-probability regions, capturing complex parameter interactions that ABC-MCMC fails to identify.

The trace plots further confirm the superiority of ABC-SMC in posterior exploration. ABC-SMC particles exhibit rapid transitions and broad fluctuations, indicating efficient mixing and reduced autocorrelation, whereas ABC-MCMC traces show high autocorrelation, slow transitions, and poor mixing. For some parameters, such as m, the MCMC trace remains nearly flat, suggesting trapping in a local mode and limited exploration of the posterior space.

Posterior predictive checks provide additional evidence of ABC-SMC's improved performance. Both methods successfully reproduce the general epidemic trajectory, including the initial growth and eventual plateau of infections. However, ABC-SMC shows better agreement during the mid-epidemic phase, reflecting more accurate parameter estimation, while ABC-MCMC tends to predict an earlier plateau, likely due to biased parameter estimates resulting from limited posterior exploration.

In summary, ABC-SMC demonstrates superior performance across all aspects evaluated, making it a more robust method for complex epidemic modelling. Its enhanced ability to explore multimodal posterior distributions and produce accurate predictive trajectories makes it preferable where reliable parameter estimation is crucial.

CONFLICT OF INTERESTS

The authors declare that there is no conflict of interests.

REFERENCES

[1] World Health Organization, World Malaria Report 2024, (2024). https://www.who.int/teams/global-malaria-programme/reports/world-malaria-report-2024.

[2] African Leaders Malaria Alliance, 2024 Africa Malaria Progress Report, (2024). https://alma2030.org/heads-of-state-and-government/african-union-malaria-progress-reports/2024-africa-malaria-progress-report.

[3] Kenya National Bureau of Statistics, Kenya Demographic and Health Survey, 2022. https://www.knbs.or.ke/reports/kdhs-2022.

[4] Severe Malaria Observatory, Kenya: Malaria Facts, https://www.severemalaria.org/countries/kenya.

[5] R. Ross, The Prevention of Malaria, John Murray, 1911.

[6] G. Macdonald, G. Macdonald, The Epidemiology and Control of Malaria, Oxford University Press, (1957).

[7] S. Mandal, R.R. Sarkar, S. Sinha, Mathematical Models of Malaria - a Review, Malar. J. 10 (2011), 202. https://doi.org/10.1186/1475-2875-10-202.

[8] A.O. Sharon, S.C. Maina, C.O. Odhiambo, S. Mwalili, Bayesian Reasoning and Sir Malaria Models, Commun. Math. Biol. Neurosci. 2025 (2025), 80. https://doi.org/10.28919/cmbn/9247.

[9] M.A. Beaumont, J. Cornuet, J. Marin, C.P. Robert, Adaptive Approximate Bayesian Computation, Biometrika 96 (2009), 983–990. https://doi.org/10.1093/biomet/asp052.

[10] S.A. Sisson, Y. Fan, M.M. Tanaka, Sequential Monte Carlo Without Likelihoods, Proc. Natl. Acad. Sci. 104 (2007), 1760–1765. https://doi.org/10.1073/pnas.0607208104.

[11] P. Del Moral, A. Doucet, A. Jasra, An Adaptive Sequential Monte Carlo Method for Approximate Bayesian Computation, Stat. Comput. 22 (2011), 1009–1020. https://doi.org/10.1007/s11222-011-9271-y.

[12] F.V. Bonassi, M. West, Sequential Monte Carlo with Adaptive Weights for Approximate Bayesian Computation, Bayesian Anal. 10 (2015), 171–187. https://doi.org/10.1214/14-ba891.

[13] S. Filippi, C.P. Barnes, J. Cornebise, M.P. Stumpf, On Optimality of Kernels for Approximate Bayesian Computation Using Sequential Monte Carlo, Stat. Appl. Genet. Mol. Biol. 12 (2013), 87–107. https://doi.org/10.1515/sagmb-2012-0069.

[14] A.A. Alahmadi, J.A. Flegg, D.G. Cochrane, C.C. Drovandi, J.M. Keith, A Comparison of Approximate Versus Exact Techniques for Bayesian Parameter Inference in Nonlinear Ordinary Differential Equation Models, R. Soc. Open Sci. 7 (2020), 191315. https://doi.org/10.1098/rsos.191315.

[15] G. Storvik, A. Diz-Lois Palomares, S. Engebretsen, et al. A Sequential Monte Carlo Approach to Estimate a Time-Varying Reproduction Number in Infectious Disease Models: The COVID-19 Case, J. R. Stat. Soc. Ser.: Stat. Soc. 186 (2023), 616–632. https://doi.org/10.1093/jrsssa/qnad043.

[16] A.M. Stuart, Inverse Problems: a Bayesian Perspective, Acta Numer. 19 (2010), 451–559. https://doi.org/10.1017/s0962492910000061.

[17] R. Ghanem, D. Higdon, H. Owhadi, Handbook of Uncertainty Quantification, Springer, Cham, 2016. https://doi.org/10.1007/978-3-319-11259-6.

[18] D. Calvetti, M. Dunlop, E. Somersalo, A. Stuart, Iterative Updating of Model Error for Bayesian Inversion, Inverse Probl. 34 (2018), 025008. https://doi.org/10.1088/1361-6420/aaa34d.